
Effect of local hydroclimate on phytoplankton groups in the Charente estuary

Guesdon Stephane ^{1,a}, Stachowski-Haberkorn Sabine ^{2,a,*}, Lambert Christophe ³, Beker Beatriz ³, Brach-Papa Christophe ⁴, Auger Dominique ⁴, Bechemin Christian ⁵

¹ Ifremer, Laboratoire Environnement Ressource des Pertuis Charentais, Ifremer, avenue de Mus de Loup, 17390 La Tremblade, France

² Ifremer, Laboratoire d'écotoxicologie, rue de l'île d'Yeu, BP 21105, F-44311 Nantes cedex 03, France

³ Laboratoire des Sciences de l'Environnement Marin (LEMAR), UMR6539 Institut Universitaire Européen de la Mer (IUEM), Université de Bretagne Occidentale (UBO) Place Nicolas Copernic, 29280 Plouzané, France

⁴ Laboratoire de Biogéochimie des Contaminants Métalliques, Ifremer, rue de l'île d'Yeu, BP 21105, 44311 Nantes cedex 03, France

⁵ Ifremer, Laboratoire Environnement Ressource des Pertuis Charentais, Ifremer, BP7, 17137 L'Houmeau, France

* Corresponding author : Sabine Stachowski-Haberkorn, email address : Sabine.Stachowski.Haberkorn@ifremer.fr

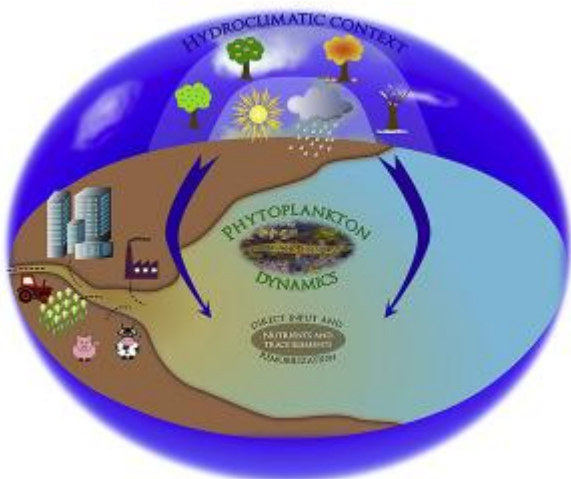
^a These first authors contributed equally to this article.

Abstract :

This study aimed to describe seasonal variations of phytoplankton abundances in relation to the physical and chemical (nutrients and metals) environment under the influence of freshwater input in the Charente river estuary (Marennes-Oléron bay, France) over three years, from 2011 to 2014. Phytoplankton abundances were determined using microscopy and flow cytometry. Considering high frequency temperature and salinity data, breakpoints in each series led to the identification of two local hydroclimatic periods: the first (2011 and early 2012) being warmer and higher in salinity than the second (from spring 2012 to the beginning of 2014). A multiblock PLS analysis highlighted the significant contribution of the physical environment (temperature, salinity and Photosynthetically Active Radiation (PAR)) on phytoplankton abundances. Two partial triadic analyses (PTA) were run in order to visualize seasonal variations of i) phytoplankton groups and ii) nutrients and trace elements, irrespective of spatial gradient: picoeukaryote occurrence showed a difference between year 2011 and the years 2012 and 2013 (as did cadmium, nickel and silica levels). However, both PTA revealed greater differences between year 2013 and the years 2011 and 2012, as shown by occurrences of cryptophytes, dinoflagellates and nanoeukaryotes, as well as copper and phosphate levels. These results showed a shift between the hydroclimate breakpoint and some phytoplankton responses, suggesting that their development and succession might depend on conditions early in the year. Finally, a STATICO analysis was performed on the paired PTA in order to examine the relations of phytoplankton with nutrients and metals more closely. Most phytoplankton groups were represented on the first axis, together with cadmium on the one hand, and nitrates, silica and nickel on the other. This

analysis revealed the separation of phytoplankton groups on the second axis that represented phosphates and copper. Hydroclimatic conditions and the nature of freshwater inputs, especially phosphates and copper content, might be key factors driving phytoplankton structure in the Charente estuary.

Graphical abstract



Highlights

► Phytoplankton groups were studied in the Charente estuary for three years. ► The local hydroclimate (temperature and salinity) showed two distinct periods. ► Phytoplankton dynamics were mainly driven by their physical environment (temperature). ► The diatom spring bloom was fairly consistent. ► Phytoplankton structure could be linked to copper and phosphates.

Keywords : Hydroclimate, Estuary, Phytoplankton, Size composition, Nutrients, Trace metals

1. Introduction

Approximately 40% of the world population inhabits coastal and estuarine areas (MEA, 2005), concentrating human activities that cause damage to marine ecosystems (Halpern et al., 2008). Human activities exert intensive stresses on marine ecosystems, including chemical contamination (urbanization, agriculture, industry) and disturbances caused by the exploitation of marine resources (fishing, aquaculture, aggregate extraction, etc.) (Nogales et

al., 2011). Coastal ecosystems are among the world's most productive ecosystems and provide many vital ecological services that need to be preserved (Costanza et al., 1997; MEA, 2005; Barbier et al., 2011; Liqueste et al., 2013), such as shelters for reproduction and nurseries for marine species. Their role in nutrient cycling is essential, depending on the quantity and quality of terrigenous inputs, as nutrients act directly on the lowest trophic levels and induce changes in the composition of the microbial community (Nogales et al., 2011). Phytoplankton plays a major role in microbial communities, where it is responsible for primary production and represents the main trophic resource for higher trophic levels.

Natural phytoplankton communities have been greatly studied worldwide, in freshwater, coastal (Gasiunaite et al., 2005; Aktan, 2011) and estuarine environments (Muylaert et al., 2009; Rochelle-Newall et al., 2011). Classic analysis of phytoplankton communities using microscopy allows counts and determination of taxa to class or species level (Cloern and Dufford, 2005; Domingues et al., 2011; Hall et al., 2013; Paerl et al., 2014; Harding et al., 2015). Such studies can be used to describe the effect of environmental variables (nutrients, light) on phytoplankton dynamics and community structure evolution (Hall et al., 2013; Paerl et al., 2014). As shown by Harding et al. (2015), the seasonal pattern in the northern hemisphere has spring or summer blooms that are influenced from year to year by climatic events. Global change, especially temperature increase, is a key question in the study of phytoplankton communities (Edwards and Richardson, 2004; Morán et al., 2010). For instance, Thomas et al. (2012) demonstrated that temperature could impact the spatial distribution of communities, and thus cause changes in diversity.

Studies that deal with phytoplankton community evolution, dynamics and structure in space and time while considering different cell-size groups (from pico- to microplankton) are scarce (Sin et al., 2000; Huete-Ortega et al., 2011; Cerino et al., 2012), but are necessary to improve our understanding of ecosystem function based on phytoplankton communities (Segura et al.,

2013; Marañón, 2015). The importance of understanding what factors drive phytoplankton communities and how they evolve is emphasized by their place in EU regulations (Water Framework Directive, WFD 2000/60/CE and Marine Strategy Framework Directive, MSFD 2008/56/CE) among the indicators of water mass ecological status. Lugoli et al. (2012) suggested the use of phytoplankton size-classes as an indicator of anthropogenic impact in marine and transition areas. However, as stated by Garmendia et al. (2013), many attributes of phytoplankton need to be considered before it is possible to develop a robust and sensitive indicator. There is thus a need to investigate whole phytoplankton communities, together with their physical and chemical environment, in order to define the baseline variations of all the parameters. Only such complete approaches will make it possible to discriminate for 'events' caused by environmental disturbances.

In coastal areas, estuaries are transition areas between freshwater and marine ecosystems, subjected to strong anthropogenic pressure but achieving high productivity thanks to freshwater inputs. Among the most productive coastal areas on the French Atlantic coast, Marennes-Oléron bay (Région Poitou-Charentes, south-west France) is the top oyster producing area in France (Gouletquer and Héral, 1997): out of the 101 000 t of oysters produced in France in 2011/2012, 39 000 t were produced in Poitou-Charentes (CNC, 2014). This high oyster production relies mainly on primary production, which is largely due to phytoplankton. Nutrients are supplied by the Charente river, which discharges into the bay contributing about 90% of the freshwater input during summer (Ravail-Legrand et al., 1988). These nutrients were estimated to contribute annually to a primary production of $185 \text{ gC.m}^{-2}.\text{an}^{-1}$ in the water column of Marennes-Oléron bay (Struski and Bacher, 2006), underlining their importance for phytoplankton development.

The first aim of this study was to describe the seasonal variations of phytoplankton abundances in the transition area of the Charente estuary, during three years of monitoring

(2011-2014). The second purpose was to understand to what extent local hydroclimate and freshwater inputs (nutrients and trace elements) drive phytoplankton abundances in this specific environment.

2. Materials and methods

2.1 Sampling site and strategy

The Charente estuary (45°70'N, 1°00'W) is located on the Atlantic coast of south-west France. The Charente river is 360 km long with a catchment basin of about 10 000 km², mostly occupied by agriculture (75% of its surface, Agreste 2010). The flow amplitude ranges from several m³.s⁻¹ to 700 m³.s⁻¹, with an average of 70 m³.s⁻¹ (Toublanc et al., 2015). The Charente estuary is a small, shallow, macrotidal estuary with a mean tidal range of 4.5 m and well-mixed waters (Toublanc et al., 2015). In addition, the asymmetric tide waves lead to continual resuspension of seabed sediments (Modéran et al., 2012). The present study was run along a transect of about 12 km that was not subject to water stratification.

Sampling campaigns were carried out every two weeks from February 2011 to January 2014, taking samples at low tide when the influence of freshwater inputs was the highest, thus allowing the quantification of trace elements. Four stations were sampled in the Charente estuary (Fig. 1): the depths of the four stations ranged from 4 to 11 m from the mean sea level (6 m for Station 1). The station the furthest upstream (Station 1: Lupin), which was located at 45.9538N -01.0544E, was equipped with multiparameter probes (YSI 6600 or NKE Smatch) that recorded continuously. The three other stations were mobile and their position was defined during each campaign depending on the salinity gradient, as follows. The most downstream station (Station 4) was defined as the place corresponding to the maximal salinity value that had occurred at high tide at Station 1 the day before. Locations of stations 2 and 3 were then defined in consequence so as to obtain a homogeneous salinity gradient between the lowest salinity value at Station 1 and the highest expected value at Station 4. At each

station, sub-surface water samples were collected using 5-L and 2.5-L Niskin bottles for subsequent analyses of nutrients, dissolved metals and phytoplankton.

2.2 *In situ* physico-chemical measurements

Station 1 (Lupin) was monitored from 2000 to 2014 as part of the SAPERCHAIS program (Guesdon et al., 2015). In this context, temperature and salinity were recorded *in situ*, just below the surface, at a high frequency resolution (every 10 minutes), using multiparameter probes (NKE SMATCH and YSI 6600). This dataset was used to analyse the local hydroclimatic context for the present study.

Throughout each campaign, a multiparameter probe (YSI 6600) was kept immersed at a depth of 1 m on the side of the vessel, using a home-made stainless steel device, in order to continuously record the following parameters from stations 1 to 4: temperature (°C), salinity, turbidity (FNU) and dissolved oxygen (mg.L⁻¹). By means of instantaneous salinity monitoring, stations 2 to 4 were sampled as soon as the previously defined target values were met. Salinity was measured using the Practical Salinity Scale.

2.3 Photosynthetically Active Radiation (PAR)

In order to take into account the influence of light on phytoplankton groups, Photosynthetically Active Radiation (PAR) at 1-m depth (E_z , equation (1)) was estimated at the four stations for each campaign, using the following equations:

$$(1) E_z = E_0 \exp^{-K_{par}Z} \quad (\text{Kirk, 1985}),$$

where E_z is the PAR at the depth z (1 m in the present study); E_0 ($= I_{par}$ in equation (2)) is the PAR at the water surface; K_{PAR} is the attenuation coefficient of light defined in equation (3); Z is the depth (m);

$$(2) I_{par} = 0.45I \quad (\text{Meek et al., 1984}),$$

where I_{par} ($= E_0$ in equation (1)) is the conversion to PAR; I corresponds to the global solar radiation available at a daily interval from the La Rochelle Météo France station;

$$(3) K_{par} = 0.154TPM^{0.66} \quad (\text{Struski and Bacher, 2006}),$$

where K_{PAR} is the attenuation coefficient of light; TPM is the Total Particulate Matter ($\text{mg}\cdot\text{L}^{-1}$) determined in the samples.

2.4 Sample analyses

2.4.1 Nutrients

For nutrient measures, 2 L water were sampled at each station. Samples were kept in polycarbonate bottles, in the dark at 4°C until the return to the laboratory. At the laboratory, the water was filtered through 0.2 μm pore PTFE Millipore membranes using a plastic filtering system and a vacuum of less than 10 cm Hg. The whole apparatus and the membranes were pre-washed with 1 N hydrochloric acid and rinsed with deionized water. Filtrates were stored frozen (at -20°C) in plastic vials until analysis, except for silicate analysis, where samples were stored at 4 to 6°C to prevent silicate polymerization. Ammonia (NH_4^+) was analysed using fluorimetry after reaction with orthophthalaldehyde (OPA) and sulfite, while the other nutrients (NO_3^- , PO_4^{2-} and SiO_3^-) were measured by molecular absorption. Analyses were run using a segmented flow analyser (SFA) with the San⁺⁺ Automated Wet Chemistry Analyzer from Skalar, based on the automated continuous flow analysis procedure technique according to Aminot and Kerouel (2007).

2.4.2 Trace metals

Samples were collected manually in 250-mL polyethylene bottles (acid cleaned) that were attached to a 2-m long plastic pole. Bottles were then stored in polyethylene bags in the dark at 4°C and brought back to the laboratory within 24 h in order to perform the extraction.

Seawater samples were filtered using 0.45- μm pore size polycarbonate filters (acid cleaned, Nucleopore) under nitrogen pressure in a laboratory clean room (class 100). Filtrates were acidified (0.1%, ultrapure nitric acid 67–69%) and stored in polyethylene bags until analysis.

Acidified filtrates were then treated according to Danielsson et al. (1982), as described by Chiffoleau et al. (2002). This procedure consisted in dithiocarbamate chelate formation (ammonium 1-pyrrolidinedithiocarbamate / diethylammonium diethyldithiocarbamate, sodium salts, >97%) in water phase (100 g) buffered to pH = 5, an extraction into an immiscible organic solution (1,1,2-trichloro-1,2,2-trifluoroethane, >99%) and a back extraction using diluted nitric acid (ultrapure, 1:4, v/v). The extraction step was repeated twice. Before analysis, 1 mL of the extract was diluted to 5 mL with highly purified water (>18 M Ω).

Trace metal concentrations (Ni, Cu, Zn, Cd) in seawater extracts were determined by Q-ICP-MS (Thermo Electron Corporation, Element X series) equipped with a pumped micro-concentric nebuliser (opalmist 0.8 mL/min), a conical impact bead spray chamber with a cooling system, Pt standard sampler and skimmer cones. Internal standards were systematically added to each solution to correct for instrumental drift. The ICP-MS analytical performance was checked by analysing seawater certified reference material CASS-5 or NASS-6 (National Research Council Canada, Ottawa, Canada). The analytical results obtained systematically differed from certified values by less than 15% and reproducibility was generally better than 5% for all measured metals.

2.4.3 Phytoplankton

For taxonomic analysis of phytoplankton by microscopy, 250-mL samples were collected in triplicate in glass bottles. For flow cytometry analysis, 1.5 mL were sampled from each 250-mL triplicate and put in cryotubes to which glutaraldehyde was added (final concentration 0.25%). The tubes were then vortexed and left for 10 min in the dark before being frozen in liquid nitrogen; they were then kept at -80°C until analysis. Neutral Lugol's iodine solution (2%, final concentration) was added to the remaining volume in the glass bottles in order to

preserve the microalgal cells. The bottles were then kept at room temperature in the dark until analysis.

Usually, picoplankton is considered to range from 0.2 μm to 2 μm , nanoplankton from 2 μm to 20 μm and microplankton from 20 μm to 200 μm (Sieburth et al., 1978). Given the different analyses performed for phytoplankton in the present study (microscopy and flow cytometry) and to offer greater clarity, the terms nanoeukaryotes and picoeukaryotes were used to refer to groups counted using flow cytometry (Neveux et al., 2010; Tarran et al., 2006; Tarran and Bruun, 2015), while microphytoplankton were grouped by class according to the microscopic observations. The two analyses are complementary and provide a more complete view of the phytoplankton community (Garmendia et al., 2013).

Flow cytometry

Samples collected in 2011 were run on a FacsCalibur flow cytometer (Becton Dickinson, San Jose, CA) equipped with a 488-nm argon laser and standard filter setup (530/30 nm, 585/42 nm and 670 nm/LP). From 2012, samples were run on a FacsVerse flow cytometer (Becton Dickinson, San Jose, CA) equipped with three lasers (violet: 405 nm; blue: 488 nm; red: 640 nm) and eight filters (527/32 nm, 586/42 nm, 700/54 nm and 783/56 nm for the blue laser; 448/45 nm and 528/45 nm for the violet laser; and 660/10 nm and 783/560 nm for the red laser).

Following the methods described in Marie and Partensky (2006), three main groups of photosynthetic organisms (picoeukaryotes, nanoeukaryotes and *Synechococcus* sp.) were discriminated and counted in the samples on the basis of their optical characteristics and, particularly, their natural red fluorescence (>670 nm using the FacsCalibur and 700/54 nm using the FacsVerse), orange fluorescence (585/42 nm using the FacsCalibur and 586/42 nm using the FacsVerse), relative size and complexity given by the forward and side scatter, respectively, on both cytometers. Data from FacsCalibur were analysed using the WinMDI 2.8 software (Joe Trotter) and those from the FacsVerse device with the BD FACSuite software

application V1.0.5. Abundances of groups in the samples were estimated using the method from Marie et al. (2001) with the FacsCalibur, and using the Flow Sensor device of the FacsVerse flow cytometer. However, the use of the Flow Sensor device led to an overestimation of cellular concentrations with the FacsVerse due to inaccurate volume measurements, which were linked to salinity. To avoid this bias, a relationship was established between salinity and the volumes analysed that made it possible to apply a suitable correction for the samples from different salinities. Due to the very high suspended matter content at Station 1, samples from this station could not be adequately analysed by flow cytometry.

Microscopic identification

Determination and quantification of phytoplankton cells were carried out at the species level. In the present study, due to the requirements of the data analyses performed, species counts were aggregated into classes (chlorophytes: Chloro; cryptophytes: Crypto; diatoms: Diatom; dinoflagellates: Dino; prymnesiophytes: Prymnesio). Depending on the detritic particle content, which could sometimes be very high and interfere with cell recognition, one or several sub-samples of 5 to 50 mL were settled in an Utermöhl settling chamber (Hasle, 1978) and counted using a Wild M40 phase contrast inverted microscope. Rose Bengal was used to highlight organic particles. Counts were carried out on the partial or whole bottom surface of the chamber, depending on the size and abundance of the species (Lund et al., 1958), at $\times 200$ to $\times 400$ magnification. When possible, 400 cells were counted to ensure that the error in estimation of cellular abundance remained within the limits of $\pm 10\%$ (Uehlinger, 1964).

Due to the very high suspended matter content at Station 1, count reliability was reduced: most counts indicated low abundances or even the absence of phytoplankton at this station. As flow cytometry data were also missing for this station, the results from Station 1 were not included in the data analyses.

2.5 Data analyses

In order to analyse the local hydroclimate in the most upstream station, temperature and salinity time series (daily aggregation from continuous data with 10–15 min frequency) were transformed to daily regular time series by filling gaps using (1) a model established from smoothed atmospheric temperature (2-day lag) from Chassiron Météo France station (SYNOP database) ($R^2 = 0.95$, p -value < 0.0001), and (2) modelled salinity data from flow data of Charente ($R^2 = 0.89$, p -value < 0.0001), respectively. Breakpoints were identified from deseasonalized time series of temperature and salinity by sequential estimation via a bisection algorithm based on the measurement of divergence between two dataset distributions (nonparametric method). The R package *ecp* (James and Matteson, 2013) was used to establish dates of change. Annual means calculated from regularized series made it possible to position the three years of study in the historical series (2000–2013).

Correlations of the physical environment (temperature and salinity) with nutrients and trace elements were calculated using Mann–Kendall correlation coefficients.

For the analysis of chemical elements and phytoplankton abundances, Kruskal-Wallis tests were performed to test for spatial variability (based on the different stations monitored) and temporal variability between months (data for each month were compared with each other regardless of year).

The relations between the abundance of phytoplankton groups and their environment were explored and modelled by the multiblock Partial Least Square (mbPLS) method (Bougeard et al., 2011). MbPLS makes it possible to explain a block of variables (Y_1, \dots, Y_K being the abundances of each phytoplankton group) by a large number of explanatory variables organized in K meaningful blocks (X_1, \dots, X_K), in this case three blocks: physical environment (temperature, salinity, turbidity, PAR), nutrients (NH_4^+ , NO_3^- , PO_4^{2-} , SiO_3^- , N/P, Si/N) and metals (Ni, Cu, Zn, Cd). Bootstrapping simulations (in this case 5000) were applied

to the main predictive parameters, i.e. cumulated Variable Importance Index and cumulated Block Importance Index, to provide associated confidence intervals (95%). MbPLS was also performed using the *ade4* R package (Dray and Dufour, 2007).

Seasonal stability of phytoplankton blooms and their intensity were studied with Partial Triadic Analysis (PTA). PTA is based on Principal Component Analysis and allows the analysis of a datacube (phytoplankton groups \times months \times years), seen as a sequence of two-way tables in a three-step procedure: the interstructure, the compromise and the intrastucture analyses; the interstructure offers an ordination of the three years of study and an overall seasonal typology; the compromise makes it possible to see the common structures of the three years of study, with regard to phytoplankton groups and months; the intrastucture provides a detailed description of the deviations from the common model for each year. Thioulouse and Chessel (1987) and Thioulouse et al. (2004) provided a detailed description of this analysis. PTA was run using the R package *ade4* (Dray and Dufour, 2007). The same analysis was used with the nutrient and trace element dataset.

To explain the structure in common between phytoplankton group abundances and levels of nutrients and trace elements, a STATICO analysis was performed using each datacube (phytoplankton group abundances \times months \times years; nutrients and trace element concentrations \times months \times years). The STATICO method is a Partial Triadic Analysis on the sequence of cross product tables resulting from the co-inertia between phytoplankton group abundances and nutrient and trace element concentrations for each year (Thioulouse, 2011). Therefore, the STATICO analysis proceeds with the same three steps as the PTA described above.

All analyses and plots were performed with R Software (R Core Team, 2014).

3. Results

3.1 Local hydroclimatic context

3.1.1 Situation of the study period in the continuity of the last decade

The high frequency acquisition (every 10 min) of temperature and salinity data at Station 1 since the year 2000 made it possible to situate the study period (2011–2014) in the context of the last fourteen years. The smoothed deseasonalized daily temperatures obtained from these historical data ranged from 14.1°C to 15.1°C (Fig. 2a) in the 2000–2011 period, while the range during the study was 13.6–14.8°C and showed a continuous significant decreasing trend ($\tau = -0.24$, $p < 0.0001$, Mann–Kendall). For salinity at Station 1 (Fig. 2b), the 2000–2011 amplitude ranged from 14.0 to 22.7, while the amplitude encountered during the study was 14.0–22.3, and also showed a strong, continuous and significant drop over a short period ($\tau = -0.46$, $p < 0.0001$, Mann–Kendall). Both parameters, but especially salinity, fluctuated over periods of several years during the monitored period as a whole and exhibited a marked drop during the period of the present study.

3.1.2 Identification of major events during the study period

The decreasing pattern of temperature and salinity observed during the study prompted us to check for any notable events in the deseasonalized series of these parameters, which we did using a statistical analysis based on divergence between distributions. The first breakpoints in each of the series were identified in 2012: in February for temperature (Fig. 2c) and at the end of April for salinity (Fig. 2d). To each side of these points lay periods with different local hydroclimatic conditions, with a 2–3 month delay between temperature and salinity. The first period, from January 2011 to spring 2012, was characterized by higher temperatures ($>1^\circ\text{C}$) and higher salinities (>5), similar to the overall trend observed in 2011; the second period, from spring 2012 to the end of 2013, exhibited lower temperatures and salinities.

3.1.3 Seasonal variations between years during the study

Mean annual temperature and salinity in the three years 2011, 2012 and 2013 at Lupin (Station 1) were compared to the distribution of temperature and salinity over the last 13 years (Fig. 3a and 3b, respectively). Year 2011 had extremely high mean temperature and salinity, compared with the 2000–2013 period. More precisely, temperatures were warmer in spring, late summer and autumn 2011 (Fig. 3c), corresponding to very high salinity values at nearly the same time (Fig. 3d). The year 2012 appeared average compared with the previous 13 years (Fig. 3a and 3b). Temperature showed a large drop during February (Fig. 3c), and the end of the year was slightly colder than the 13-year period of automatic recordings. Salinity was highly variable over the year, showing many irregularities, with large drops, especially in May, early autumn and winter (Fig. 3d). Year 2013 had quite low mean temperature and salinity values compared with the previous 13 years (Fig. 3a and 3b, respectively). Temperatures were colder during late spring, early summer and late autumn (Fig. 3c), with several periods where salinity was very low (winter, spring, early summer and late autumn, Fig. 3d).

3.2 Spatial and temporal variations of phytoplankton and their environment

3.2.1 Physico-chemical environment

Along the studied section of estuary, all nutrients and metals showed significant gradients, with higher concentrations upstream (except cadmium) and lower ones downstream (Fig. 4) (Table 1, $p < 0.05$). The gradients were more pronounced for the most concentrated nutrients, starting with nitrates (mean 65–308 μM from down- to upstream) and silica (mean 35–146 μM from down- to upstream). Phosphates had a shallower gradient (mean 0.9–1.9 μM from down- to upstream), as did metals (means 0.59–0.96 $\mu\text{g}\cdot\text{L}^{-1}$ for Cu, 0.37–0.59 $\mu\text{g}\cdot\text{L}^{-1}$ for Ni and 0.021–0.017 $\mu\text{g}\cdot\text{L}^{-1}$ for Cd, from down- to upstream).

In addition, salinity showed significant negative links with nitrates ($\tau = -0.80$, $p < 0.001$, Mann–Kendall), silica ($\tau = -0.67$, $p < 0.001$, Mann–Kendall), copper ($\tau = -0.36$, $p < 0.001$) and nickel ($\tau = -0.52$, $p < 0.001$, Mann–Kendall), while a positive link was noted for cadmium ($\tau = 0.43$, $p < 0.001$, Mann–Kendall). Significant positive links were also shown between temperature and phosphates ($\tau = 0.24$, $p < 0.001$, Mann–Kendall), copper ($\tau = 0.175$, $p = 0.006$) and cadmium ($\tau = 0.29$, $p < 0.001$, Mann–Kendall).

3.2.2 Phytoplankton abundances

The abundances of eight phytoplankton groups were recorded from upstream (Station 2) to downstream (Station 4), throughout the study (Fig. 5). The most abundant groups were picoeukaryotes (Pico), nanoeukaryotes (Nano) and *Synechococcus* sp. (Synecho), with densities around $1\text{--}10 \times 10^6$ cell.L⁻¹; these groups were also omnipresent in the samples throughout the years of the study. Of the other groups, diatoms (Diatom) were the most abundant and frequently present, with maximal densities around 1×10^6 cell.L⁻¹. Cryptophytes (Crypto) and dinoflagellates (Dino) were less abundant but present during certain periods of the year. Chlorophytes (Chloro) and prymnesiophytes (Prymnesio) were only found occasionally during the study and at very low concentrations (except during blooms).

Spatial variability of abundances was significant for most of the groups (Table 2, p -value spatial < 0.05), except for Pico, Prymnesio and Chloro: picoeukaryote abundances were similar all along the salinity gradient (Fig. 5), whereas Prymnesio and Chloro presence was rare (occurrence $< 10\%$, Table 2) and seemed unaffected by salinity. Synecho, Diatom, Dino and Crypto were rather abundant in downstream waters (Fig. 5), while Nano abundances were higher in upstream waters.

The evolution of abundances through time was considered at the monthly scale. Significant differences were shown for half of the groups (p -value month, Table 2): Pico, Nano, Diatom and Dino abundances were higher during the spring to autumn period (Fig. 5), with Diatom

abundances being particularly high in spring. For the other groups, no significant differences were detected between months (Table 2). *Synecho* were present at high abundances in all the years, although a dramatic drop was seen during spring 2012 (Fig. 5).

Finally, abundance data highlighted: i) groups with variable abundances in space and time (*Nano*, *Diatom* and *Dino*); ii) groups varying only in space (*Synecho* and *Crypto*); and one group with variations only at the monthly scale (*Pico*). The very low occurrence of *Chloro* and *Prymnesio* during the study (<10% in each station) was not sufficient to draw conclusions about their variability in time, these groups were thus excluded from further analyses.

3.2.3 Importance of physico-chemical parameters for overall phytoplankton abundances

In order to determine which variables contributed the most to the variations in phytoplankton abundances, a multiblock PLS analysis was performed. The group of dependent variables (each phytoplankton group abundance) was explained using three categories of explanatory variables (Table 3): physical environment, nutrients and metals. The multiblock PLS method explained 71.3% of phytoplankton abundance variability, corresponding mainly to the physical environment category (53.1% [47.1–59.0%]_{95%}), followed by nutrients (27.7% [24.8–30.6%]_{95%}) and metals (19.2% [14.1–24.3%]_{95%}) (Table 3).

The detailed contributions of each variable indicate that temperature, PAR and salinity significantly contributed to the overall phytoplankton abundances, showing the prevailing dependence of phytoplankton on the effect of climate on hydrology. Within the nutrients and metals categories, ammonia and zinc were the smallest contributors (both <1%); they were thus not considered in further analyses.

3.3 Integration of variations observed during the study: between-year differences in seasonality

Variations in dissolved substances and phytoplankton group abundances through the seasons and years were analysed separately from salinity, using values from all the stations, which were averaged and aggregated per month.

3.3.1 Phytoplankton groups

A PTA was run in order to visualize the seasonal variations of phytoplankton groups during the study (Fig. 6). As shown by the interstructure, which represents the phytoplankton structure over the years (Fig. 6a), the abundances globally indicated different patterns between the year 2013 and the years 2011 and 2012. This can be seen more precisely on the intrastructure (Fig. 6b), where the first two axes that allow the description of phytoplankton seasonality represent 83.5% of inertia (Fig. 6c). The X-axis shows the opposition between winter on the right and summer on the left (season tags, Fig. 6b), and the Y-axis corresponds to the opposition between spring (at the top) and autumn (at the bottom). For a given group, the seasonal occurrence is represented by the positioning of points corresponding to each year: when they are relatively close to each other, the seasonal occurrence of the group is quite steady. As for abundance (Fig. 6d), groups shown by longer arrows are better represented. Abundances can be ranked by projection of each year's points onto their main axis (Fig. 6b). Diatom and Pico appeared regularly at the same time of the year during the study: in spring and summer, respectively. Pico exhibited the same abundance levels over the years, while Diatom were more abundant during 2012. Both of these groups were well represented in the analysis (Fig. 6d), as were Nano and Dino. Nano and Dino exhibited opposite temporal trends (Fig. 6b): even though their respective occurrences were centred on summer, Dino occurred earlier in the year in 2011 and 2012, with lower abundances. Dino occurred later in summer in 2013 with much higher abundances. Nano occurred later in 2012 compared with 2011 and, especially, 2013 and were most abundant in 2012 (such as Diatom), whereas their abundances were much lower in 2013. Synecho and Crypto abundances are not

well represented on the vector plan (Fig. 6d); nevertheless, they showed high variability in occurrence during the study. For *Synecho*, year 2012 can be noted as opposite to 2011 and 2013. *Crypto* were unstable through the seasons, showing an opposition between years 2011 and 2012 on the one hand, with an occurrence early in the year (spring), and 2013 on the other, when the group appeared later (autumn).

3.3.2 Nutrients and trace metals

Seasonal variations in nutrients and trace metals were analysed in the same way as the phytoplankton groups (PTA, Fig. 7). The analysis explained almost all the variability of the dataset with the two first axes (95%, Fig. 7a). The data structure over the years revealed a similarity between the years 2011 and 2012, while 2013 seemed different (Fig. 7b). The compromise indicated that, overall, the variables were well represented by the analysis (data not shown). Most of the elements were measured between summer and winter, except nitrates, which were predominant between winter and spring (Fig. 7c). Depending on the elements, some years were close to each other and exhibited higher concentrations, such as 2011 and 2012 for Cu and phosphates (between summer and autumn), and 2012 and 2013 with higher concentrations for Ni and Si (at the end of the year). For Cd, the highest concentrations appeared in late summer in 2011.

3.4 Relations between phytoplankton groups, nutrients and trace metals

The simultaneous analysis of paired data cubes (phytoplankton groups \times months \times years with nutrients and metals \times months \times years) made it possible to visualize the links between phytoplankton and dissolved substances in their environment (Fig. 8). The first two axes of the STATICO analysis represent 96% of inertia (Fig. 8a). Five out of six phytoplankton groups (not Cryptophytes) are represented on the left part of the first axis, accounting for 74.9% of the variability (Fig. 8b). This first axis also separates four out of the six dissolved substances (nitrates, silica and nickel on the right, cadmium on the left). The second axis

(21% of inertia, Fig. 8a) that represents copper and phosphates, shows the contrast between the phytoplankton groups, from diatoms (upper part) to picoeukaryotes (lower part). The STATICO analysis revealed that most phytoplankton group abundances are represented as opposite to nitrates, silica and nickel, while cadmium is found in the same direction. The discrimination of different phytoplankton groups on the second axis appears linked to phosphates and copper, which are significant on this axis.

4. Discussion

In the present study, hydroclimate was associated with temperature and salinity, which were continuously recorded in the station furthest upstream. These physical variables are global descriptors of water masses that integrate other variables linked to climate and hydrodynamics. They reflect the effects of atmospheric temperature and river flow, itself linked to precipitation, on the water masses. The Charente estuary is a small, shallow, macrotidal estuary where dynamics are mainly driven by tide current and the flow of the Charente river, with negligible influence of wind and no stratification of water masses (Toublanc et al., 2015).

In terms of its hydroclimatic context, the period of the present study showed amplitudes of temperature and salinity as great as those encountered during the much longer period from 2000 to 2011 (Fig. 2). This led to contrasted years; 2011 being the warmest and driest, with low terrigenous inputs to the estuary, and 2013 being cold and wet. Within the study period, two hydroclimatic periods were thus distinguished (2011 to early 2012 and early 2012 to the beginning of 2014). Temperature and salinity, as variables linked to the hydroclimate, were shown to contribute significantly to explaining variations in phytoplankton group abundances during the study, together with PAR. Climate is recognized as playing a major role in phytoplankton community ecology (Cloern and Dufford, 2005) and structure (Hall et al., 2013), acting on different spatial and temporal scales (Harding et al., 2015). In the present

study, the analysis showed that local hydroclimate contributed to variations in phytoplankton group abundances in the transition area of an estuary over a three year period.

When considering more precisely at phytoplankton groups and seasonal variability over years, it appeared that group responses did not necessarily match up with the two hydroclimate periods discerned. The only group that exhibited a different pattern in 2012 and 2013 (after the break) compared with 2011 was the picoeukaryotes (PTA results, Fig. 6): this group was shown to be quite ubiquitous along the salinity gradient (Fig. 5) and its phenology might mostly be dependent on temperature trends, showing reactivity to changes. In contrast, nanoeukaryotes, dinoflagellates and cryptophytes mostly showed the same patterns in 2011 and 2012, with differences in 2013. These groups did not seem directly affected by the change in hydroclimate, but instead exhibited a delayed response that might have been driven by additional parameters. Their spatial variations are related to the effect of the salinity gradient and thus to the influence of freshwater inputs (Cloern and Duffort 2005). The pattern observed in 2012, similar to 2011, would have been linked to the salinity context of the early part of the year (before May), leading to their delayed response to the breakpoint in hydroclimate characteristics. In spite of differences in diatom bloom intensities between years (Fig. 6), the occurrence of a spring bloom was quite regular, most probably as a result of lengthening photoperiod after winter (Edwards and Richardson, 2004), suggesting only a weak influence of freshwater inputs on their time of appearance. The most intense bloom was observed at the end of the first hydroclimate period, before May 2012 (Fig. 5). At this time, freshwater inputs were lower than in spring 2013, when salinity was low corresponding to enhanced freshwater inputs, accompanied by a very weak diatom bloom. This result suggests that high freshwater inputs might not favour a diatom bloom, as their development may be limited by total suspended matter (Domingues et al, 2011) even when enough nutrients are available (Cloern, 2001).

Indeed, in this estuary, nutrient availability relies partly on anthropogenic inputs, particularly those originating from seasonal activities (e.g. agriculture), with inputs (mostly nitrates and silica) being linked to rainfall pattern and thus to salinity (Treguer et al., 2014). Among other dissolved substances, a positive correlation with temperature revealed some relations with enhanced remineralization from sediments in warm conditions (phosphates) (Serpa et al., 2007) together with modification of the particulate-dissolved equilibrium/speciation of metals linked to temperature and/or salinity (copper and cadmium) (Zhao et al., 2013). Dissolved substance concentrations measured do not only reflect hydroclimate influence, but also integrate the interactions with organisms via consumption and release that occur for nutrients and metals (Sunda, 2012). In spite of this, the variations in some substances are responsive to hydroclimate: silica and nickel concentrations are even higher when freshwater inputs are strong (Fig. 4), e.g. during the winters and periods when salinity was unusually low in 2012 and 2013 (end of spring and summer). In contrast, cadmium exhibited higher dissolved concentrations when salinity was high, especially during summer–autumn 2011 (Zhao et al., 2013).

The STATICO analysis between dissolved substances and phytoplankton abundances revealed that substances responsive to hydroclimate variations (silica, nickel, nitrates and cadmium) were associated with the abundances of most phytoplankton groups (except cryptophytes). This result revealed the common elements favourable to phytoplankton occurrence in the Charente estuary, where nitrates have been shown to be non-limiting (Struski, 2005). Phytoplankton groups were separated on a second axis corresponding to copper and phosphates, suggesting that these have a structuring role. These two substances showed similar concentration patterns to each other in 2011 and 2012 compared with a differing pattern in 2013, with a delay between the hydroclimate breakpoint and their variations. This pattern difference was also noticed for groups of nanoeukaryotes,

dinoflagellates and cryptophytes. Their positive link with temperature also illustrates the structuring effect of this hydroclimate-related parameter (Hall et al., 2013; Paerl et al., 2014). Such as nutrients, trace metals appeared to be linked to phytoplankton abundances and structure (Sunda, 2012), suggesting their importance in phytoplankton dynamics. Depending on their concentrations (Chakraborty et al., 2010), they can act as essential nutrients involved in biological processes such as photosynthesis and respiration (Sunda, 2012; Twining and Baines, 2013), or as contaminants (Debelius et al., 2009) to phytoplankton. At the concentrations measured in the present study, dissolved copper might act as a nutrient rather than a contaminant (Chakraborty et al., 2010). To our knowledge, very few studies dealing with phytoplankton structure and dynamics include the measurement of dissolved trace elements but, as demonstrated by Rochelle-Newall et al. (2011), some organometallic species (Hg and Sn) can be important factors determining phytoplankton structure in impacted estuaries. In addition, in mesocosm experiments using phytoplankton communities from an estuary supplied with nutrients and/or trace metals (including Cd and Cu), Riedel et al. (2003) highlighted the complexity of chemical and biological interactions, which resulted in different kinds of effects on the phytoplankton groups. For instance, trace elements often caused phytoplankton assemblages to shift to smaller size classes. However, these effects depended on the phytoplankton community composition and on temporal and spatial patterns in nutrient and trace metal loadings. In the natural environment, it remains difficult to assess to what extent such substances contribute to phytoplankton dynamics in differently impacted but highly productive estuarine areas.

Together with hydroclimate and nutrients, trace metals might be key components driving phytoplankton abundance and structure over time and space in estuaries, and therefore deserve more thorough investigation in studies dealing with phytoplankton dynamics in such small but highly variable areas.

5. Conclusions

In the present study, the use of complementary techniques to count phytoplankton (flow cytometry together with microscopy) made it possible to consider the whole community in order to study the dynamics of different groups in the Charente estuary. The characterization of hydroclimate during our study (2011–2014) depicted in a longer context (2000–2014) highlighted strong temperature and salinity decreases over a short time. The climate breakpoint that occurred during the study was accompanied by an immediate shift in picoeukaryote abundance pattern, while other groups (nanoeukaryotes, dinoflagellates and cryptophytes) exhibited delayed responses to these changes. Diatoms showed relatively steady seasonality and seemed unaffected by hydroclimate variations or inter-annual fluctuations in dissolved substances. Overall, the physical environment (especially temperature) was shown as mainly contributing to phytoplankton abundances and structure, acting directly and indirectly (through interactions with several nutrient availability, particularly in summer) on phytoplankton. The influence of nutrients and trace metals appeared more pronounced around summer, when occurrence and abundances were more variable. Phosphates and copper were also shown to play a significant role in phytoplankton structure, highlighting the interest of considering trace elements when studying phytoplankton ecology. In the context of global change (Pachauri et al., 2014), hydroclimate modifications are expected to induce shifts in phytoplankton dynamics and cause profound structural changes in these communities.

Acknowledgements

This study was supported by the research program “Assessing and reducing environmental risks from pesticides” funded by the French Ministry responsible for Ecology. This study also benefited from the CPER Poitou-Charentes. We would like to thank Jean Luc Seugnet, James Grizon, Larissa Haugarreau, Dominique Ménard, Julien Rouxel, Philippe Geairon, Alexandra

Duchemin, Nathalie Coquillé, Morgane Hubert and Célia Khélifi, for their involvement in the sampling campaigns. The authors thank Jean-Michel Chabirand who handled the metrology aspects of the study. The authors are grateful to Céline Vérité for performing nutrient analyses and to Gabriel Charpentier for technical assistance. From the LEMAR team, the authors thank Nelly Le Goïc and Fabienne Legrand for their technical help and Philippe Soudant, Michel Auffret, Denis De La Broise, H  l  ne H  garet, and Louis Quiniou for their involvement in the research program that funded the present work. The authors wish to thank Jean-Fran  ois Chiffolleau for his involvement in the research program and Emmanuelle Rozuel for performing trace metal analyses. We also acknowledge Florence Rivet for her help with the bibliographic research and Helen McCombie for the English correction. We also thank two anonymous reviewers for their comments, which helped us to improve the quality of this manuscript.

References

- Agreste. <http://agreste.agriculture.gouv.fr/recensement-agricole-2010/>
- Aktan, Y., 2011. Large-scale patterns in summer surface water phytoplankton (except picophytoplankton) in the Eastern Mediterranean. *Estuarine, Coastal and Shelf Science* 91, 551–558.
- Aminot, A., K  rouel, R., 2007. Dosage automatique des nutriments dans les eaux marines: m  thodes en flux continu. Ed. Ifremer, *M  thodes d’analyses en milieu marin*, 188 p.
- Barbier, E.B., Hacker, S.D., Kennedy, C., Koch, E.W., Stier, A.C., Silliman, B.R., 2011. The value of estuarine and coastal ecosystem services. *Ecological Monographs* 81, 169–193.
- Bougeard, S., Lupo, C., Le Bouquin, S., Chauvin, C., Qannari, E.M., 2011. Multiblock modelling to assess the overall risk factors for a composite outcome. *Epidemiology & Infection* 140, 337–347.

- Cerino, F., Bernardi Aubry, F., Coppola, J., La Ferla, R., Maimone, G., Socal, G., Totti, C., 2012. Spatial and temporal variability of pico-, nano- and microphytoplankton in the offshore waters of the southern Adriatic Sea (Mediterranean Sea). *Continental Shelf Research, Southern Adriatic Oceanography* 44, 94–105.
- Chakraborty, P., Babu, P.V.R., Acharyya, T., Bandyopadhyay, D., 2010. Stress and toxicity of biologically important transition metals (Co, Ni, Cu and Zn) on phytoplankton in a tropical freshwater system: An investigation with pigment analysis by HPLC. *Chemosphere* 80, 548–553.
- Chiffolleau, J.F., Auger, D., Chartier, E., 2002. Dosage de certains métaux dissous dans l'eau de mer par absorption atomique après extraction liquide-liquide. Editions IFREMER, Plouzané, France.
- Cloern, J.E., 2001. Our evolving conceptual model of the coastal eutrophication problem. *Marine ecology progress series* 210, 223–253.
- Cloern, J.E., Dufford, R., 2005. Phytoplankton community ecology: principles applied in San Francisco Bay. *Marine Ecology Progress Series* 285, 11–28.
- CNC, 2014. <http://www.cnc-france.com/La-Production-francaise.aspx>
- Costanza, R., d' Arge, R., De Groot, R., Farber, S., Grasso, M., Hannon, B., Limburg, K., Naeem, S., O'neill, R.V., Paruelo, J., 1997. The value of the world's ecosystem services and natural capital. *Nature* 387, 253–260.
- Danielsson L.-G., Magnusson B., Westerlund S., Zhang K., 1982. Trace metal determinations in estuarine waters by electrothermal atomic absorption spectrometry after extraction of dithiocarbamate complexes into freon. *Analytica Chimica Acta*, 144, 183-188.
- Debelius, B., Forja, J.M., DelValls, T.A., Lubián, L.M., 2009. Toxicity of copper in natural marine picoplankton populations. *Ecotoxicology* 18, 1095–1103.

- Domingues, R.B., Anselmo, T.P., Barbosa, A.B., Sommer, U., Galvão, H.M., 2011. Light as a driver of phytoplankton growth and production in the freshwater tidal zone of a turbid estuary. *Estuarine, Coastal and Shelf Science* 91, 526–535.
- Dray, S., Dufour, A.-B., 2007. The ade4 package: implementing the duality diagram for ecologists. *Journal of Statistical Software* 22, 1–20.
- Edwards, M., Richardson, A.J., 2004. Impact of climate change on marine pelagic phenology and trophic mismatch. *Nature* 430, 881–884.
- Garmendia, M., Borja, A., Franco, J., Revilla, M., 2013. Phytoplankton composition indicators for the assessment of eutrophication in marine waters: Present state and challenges within the European directives. *Marine Pollution Bulletin* 66, 7–16.
- Gasiunaite, Z.R., Cardoso, A.C., Heiskanen, A.S., Henriksen, P., Kauppila, P., Olenina, I., Pilkaityte, R., Purina, I., Razinkovas, A., Sagert, S., Schubert, H., Wasmund, N., 2005. Seasonality of coastal phytoplankton in the Baltic Sea: Influence of salinity and eutrophication. *Estuarine, Coastal and Shelf Science* 65, 239–252.
- Gouletquer, P., Héral, M., 1997. Marine molluscan production trends in France: from fisheries to aquaculture, in: C.L. Mackenzie Jr. (Ed.), *et al.*, *The History, Present Condition and Future of the Molluscan Fisheries of North and Central America and Europe*, vol. 3 NOAA Technical Report NMFS, Europe (1997) 129, pp. 137–164.
- Guesdon, S., Bechemin, C., Chabirand, J.-M., Verite, C., Seugnet, J.-L., Grizon, J., 2015. SAPERCHAIS-HF data and metadata. <http://dx.doi.org/10.17882/41146>.
- Hall, N.S., Paerl, H.W., Peierls, B.L., Whipple, A.C., Rossignol, K.L., 2013. Effects of climatic variability on phytoplankton community structure and bloom development in the eutrophic, microtidal, New River Estuary, North Carolina, USA. *Estuarine, Coastal and Shelf Science* 117, 70–82.

- Halpern, B.S., Walbridge, S., Selkoe, K.A., Kappel, C.V., Micheli, F., D'Agrosa, C., Bruno, J.F., Casey, K.S., Ebert, C., Fox, H.E., Fujita, R., Heinemann, D., Lenihan, H.S., Madin, E.M.P., Perry, M.T., Selig, E.R., Spalding, M., Steneck, R., Watson, R., 2008. A Global Map of Human Impact on Marine Ecosystems. *Science* 319, 948–952.
- Harding Jr., L.W., Adolf, J.E., Mallonee, M.E., Miller, W.D., Gallegos, C.L., Perry, E.S., Johnson, J.M., Sellner, K.G., Paerl, H.W., 2015. Climate effects on phytoplankton floral composition in Chesapeake Bay. *Estuarine, Coastal and Shelf Science* 162, 53-68.
- Hasle, G.R., 1978. The inverted microscope method. In: Sournia, A. (Ed.), *Phytoplankton manual*. UNESCO, Paris, pp 88–96.
- Huete-Ortega, M., Calvo-Díaz, A., Graña, R., Mouriño-Carballido, B., Marañón, E., 2011. Effect of environmental forcing on the biomass, production and growth rate of size-fractionated phytoplankton in the central Atlantic Ocean. *Journal of Marine Systems* 88, 203–213.
- James, N.A., Matteson, D.S., 2013. Ecp: An R package for nonparametric multiple change point analysis of multivariate data.
- Kirk, J.T.O., 1985. Effects of suspensoids (turbidity) on penetration of solar radiation in aquatic ecosystems. *Hydrobiologia* 125, 195–208.
- Liquete, C., Piroddi, C., Drakou, E.G., Gurney, L., Katsanevakis, S., Charef, A., Egoh, B., 2013. Current Status and Future Prospects for the Assessment of Marine and Coastal Ecosystem Services: A Systematic Review. *PLoS ONE* 8, e67737.
- Lugoli, F., Garmendia, M., Lehtinen, S., Kauppila, P., Moncheva, S., Revilla, M., Roselli, L., Slabakova, N., Valencia, V., Dromph, K.M., Basset, A., 2012. Application of a new multi-metric phytoplankton index to the assessment of ecological status in marine and transitional waters. *Ecological Indicators* 23, 338–355.

- Lund, J.W.G., Kipling, C., Le Cren, E.D., 1958. The inverted microscope method of estimating algal numbers and the statistical basis of estimations by counting. *Hydrobiologia* 11, 143–170.
- Marañón, E., 2015. Cell Size as a Key Determinant of Phytoplankton Metabolism and Community Structure. *Annual Review of Marine Science* 7, 241–264.
- Marie, D., Partensky, F., 2006. Analyse de micro-organismes marins. In: Ronot, X., Grunwald, D., Mayol, J.-F., Boutonnat, J. (Eds.), *La cytométrie en flux*. Lavoisier, Paris, pp. 211-233.
- Marie, D., Partensky, F., Vaultot, D., Brussaard, C., 2001. Enumeration of Phytoplankton, Bacteria, and Viruses in Marine Samples, *Current Protocols in Cytometry*. John Wiley & Sons, Inc., pp. 11.11.11–11.11.15.
- MEA, 2005. *Ecosystems and Human Well-being: Synthesis*, n.d. . Island Press, Washington, DC. Accessed online at www.millenniumassessment.org.
- Meek, D.W., Hatfield, J.L., Howell, T.A., Idso, S.B., Reginato, R.J., 1984. A generalized relationship between photosynthetically active radiation and solar radiation. *Agronomy Journal* 76, 939–945.
- Modéran, J., David, V., Bouvais, P., Richard, P., Fichet, D., 2012. Organic matter exploitation in a highly turbid environment: Planktonic food web in the Charente estuary, France. *Estuarine, Coastal and Shelf Science* 98, 126–137.
- Morán, X.A.G., López-Urrutia, Á., Calvo-Díaz, A., Li, W.K.W., 2010. Increasing importance of small phytoplankton in a warmer ocean. *Global Change Biology* 16, 1137–1144.
- Muylaert, K., Sabbe, K., Vyverman, W., 2009. Changes in phytoplankton diversity and community composition along the salinity gradient of the Schelde estuary (Belgium/The Netherlands). *Estuarine, Coastal and Shelf Science* 82, 335–340.

- Neveux, J., Lefebvre, J-P, Le Gendre, R., Dupouy, C., Gallois, F., Courties, C., Gérard, P., Fernandez, J-M, Ouillon, S., 2010. Phytoplankton dynamics in the southern New Caledonian lagoon during a southeast trade winds event. *Journal of Marine Systems* 82, 230–244.
- Nogales, B., Lanfranconi, M.P., Piña-Villalonga, J.M., Bosch, R., 2011. Anthropogenic perturbations in marine microbial communities. *FEMS microbiology reviews* 35, 275–298.
- Pachauri, R.K., Allen, M.R., Barros, V.R., Broome, J., Cramer, W., Christ, R., Church, J.A., Clarke, L., Dahe, Q., Dasgupta, P., others, 2014. *Climate Change 2014: Synthesis Report. Contribution of Working Groups I, II and III to the Fifth Assessment Report of the Intergovernmental Panel on Climate Change.*
- Paerl, H.W., Hall, N.S., Peierls, B.L., Rossignol, K.L., Joyner, A.R., 2014. Hydrologic Variability and Its Control of Phytoplankton Community Structure and Function in Two Shallow, Coastal, Lagoonal Ecosystems: The Neuse and New River Estuaries, North Carolina, USA. *Estuaries and Coasts*, 37, 31–45.
- R Core Team, 2014. *R: A language and environment for statistical computing.* R Foundation for Statistical Computing, Vienna, Austria. URL <http://www.R-project.org/>.
- Ravail-Legrand, B., Héral, M., Maestrini, S., Robert J.M., 1988. Incidence du débit de la Charente sur la capacité biotique du bassin ostréicole de Marenne-Oléron, *Journal de Recherche Océanographique* 13, 48–52.
- Riedel, G.F., Sanders, J.G., Breitburg, D.L., 2003. Seasonal variability in response of estuarine phytoplankton communities to stress: Linkages between toxic trace elements and nutrient enrichment. *Estuaries* 26, 323–338.
- Rochelle-Newall, E.J., Chu, V.T., Pringault, O., Amouroux, D., Arfi, R., Bettarel, Y., Bouvier, T., Bouvier, C., Got, P., Nguyen, T.M.H., Mari, X., Navarro, P., Duong, T.N.,

- Cao, T.T.T., Pham, T.T., Ouillon, S., Torrétou, J.P., 2011. Phytoplankton distribution and productivity in a highly turbid, tropical coastal system (Bach Dang Estuary, Vietnam). *Marine Pollution Bulletin* 62, 2317–2329.
- Segura, A.M., Kruk, C., Calliari, D., García-Rodríguez, F., Conde, D., Widdicombe, C.E., Fort, H., 2013. Competition Drives Clumpy Species Coexistence in Estuarine Phytoplankton. *Sci. Rep.* 3, 1037.
- Serpa, D., Falcão, M., Duarte, P., Fonseca, L.C. da, Vale, C., 2007. Evaluation of ammonium and phosphate release from intertidal and subtidal sediments of a shallow coastal lagoon (Ria Formosa – Portugal): a modelling approach. *Biogeochemistry* 82, 291–304.
- Sieburth, J.M., Smetacek, V., Lenz, J., 1978. Pelagic ecosystem structure: heterotrophic compartments of the plankton and their relationship to plankton size fractions. *Limnology and Oceanography* 23, 1256–1263.
- Sin, Y., Wetzel, R.L., Anderson, I.C., 2000. Seasonal variations of size-fractionated phytoplankton along the salinity gradient in the York River estuary, Virginia (USA). *Journal of Plankton Research* 22, 1945–1960.
- Struski, C., 2005. Modélisation des flux de matières dans la baie de Marennes-Oléron: couplage de l'hydrodynamisme, de la production primaire et de la consommation par les huîtres. PhD Thesis, Université de la Rochelle.
- Struski C., Bacher C., 2006. Preliminary estimate of primary production by phytoplankton in Marennes-Oléron Bay, France. *Estuarine, Coastal and Shelf Science* 66:323-334.
- Sunda, W., 2012. Feedback interactions between trace metal nutrients and phytoplankton in the ocean. *Front. Microbio.* 3, 204.
- Tarran, G.A., Heywood, J.L., Zubkov, M.V., 2006. Latitudinal changes in the standing stocks of nano-and picoeukaryotic phytoplankton in the Atlantic Ocean. *Deep Sea Research Part II: Topical Studies in Oceanography* 53, 1516–1529.

- Tarran, G.A., Bruun, J.T., 2015. Nanoplankton and picoplankton in the Western English Channel: abundance and seasonality from 2007-2013. *Progress In Oceanography* 137, Part B:446–455.
- Thioulouse, J., Chessel, D., 1987. Les analyses multitableaux en écologie factorielle. I: De la typologie d'état à la typologie de fonctionnement par l'analyse triadique. *Acta Oecologica Oecologia Generalis* 8, 463–480.
- Thioulouse, J., Simier, M., Chessel, D., 2004. Simultaneous analysis of a sequence of paired ecological tables. *Ecology* 85, 272–283.
- Thioulouse, J., 2011. Simultaneous analysis of a sequence of paired ecological tables: A comparison of several methods. *The Annals of Applied Statistics* 5, 2300–2325.
- Thomas, M.K., Kremer, C.T., Klausmeier, C.A., Litchman, E., 2012. A global pattern of thermal adaptation in marine phytoplankton. *Science* 338, 1085–1088.
- Toublanc F., Brenon I., Coulombier T., Le Moine O., 2015. Fortnightly tidal asymmetry inversions and perspectives on sediment dynamics in a macrotidal estuary (Charente, France). *Continental Shelf Research* 94:42-54.
- Tréguer, P., Goberville, E., Barrier, N., L'Helguen, S., Morin, P., Bozec, Y., Rimmelin-Maury, P., Czamanski, M., Grossteffan, E., Cariou, T., Répécaud, M., Quéméner, L., 2014. Large and local-scale influences on physical and chemical characteristics of coastal waters of Western Europe during winter. *Journal of Marine Systems* 139, 79–90.
- Twining, B.S., Baines, S.B., 2013. The Trace Metal Composition of Marine Phytoplankton. *Annual Review of Marine Science* 5, 191–215.
- Uehlinger, V., 1964. Etude statistique des méthodes de dénombrement planctonique. *Archives des Sciences* 17, 11–223.

Zhao, S., Feng, C., Wang, D., Liu, Y., Shen, Z., 2013. Salinity increases the mobility of Cd, Cu, Mn, and Pb in the sediments of Yangtze Estuary: Relative role of sediments' properties and metal speciation. *Chemosphere* 91, 977–984.

ACCEPTED MANUSCRIPT

TABLE 1 – Statistics of physico-chemical variables during the study (2011-2014): mean, standard deviation (SD) (N>63). The values were tested for their variability (Kruskal-Wallis) along the estuary (p-value spatial): Temperature ($^{\circ}\text{C}$), Salinity, Nitrates (μM), Phosphates (μM), Silica (μM), Copper ($\mu\text{g.L}^{-1}$), Nickel ($\mu\text{g.L}^{-1}$) and Cadmium ($\mu\text{g.L}^{-1}$). * indicates significant p-values (<0.05).

Variable	Gradient	Mean	SD	p-value spatial
Temperature	Upstream	15.245	5.594	0.9804
	v	15.168	5.500	
	v	15.040	5.315	
	Downstream	14.909	5.112	
Salinity	Upstream	9.734	6.782	0.00000*
	v	16.093	6.362	
	v	22.848	5.339	
	Downstream	29.807	4.535	
Nitrates	Upstream	307.636	155.546	0.00000*
	v	247.653	121.430	
	v	158.839	86.410	
	Downstream	64.798	57.850	
Phosphates	Upstream	1.914	1.052	0.00000*
	v	1.770	0.765	
	v	1.450	0.588	
	Downstream	0.930	0.335	
Silica	Upstream	145.838	29.416	0.00000*
	v	112.479	27.456	
	v	76.798	24.942	
	Downstream	34.985	21.194	
Copper	Upstream	0.963	0.170	0.00000*
	v	0.883	0.187	
	v	0.756	0.180	
	Downstream	0.585	0.190	
Nickel	Upstream	0.586	0.106	0.00000*
	v	0.549	0.106	
	v	0.486	0.117	
	Downstream	0.372	0.107	
Cadmium	Upstream	0.017	0.014	0.0001*
	v	0.022	0.013	
	v	0.024	0.010	
	Downstream	0.021	0.005	

TABLE 2 – Statistics of phytoplankton group abundances (abund.) during the study (2011-2014): mean, standard deviation (SD), occurrence in the samples (Occurrence in %) (N>63). The abundances were tested for their variability (Kruskal-Wallis) through time (between months: p-value month) and along the estuary (p-value spatial). * indicates significant p-values (<0.05).

Group	Gradient	Mean abund.	SD abund.	Occurrence	p-value month	p-value spatial
Picoeukaryotes	Upstream	7.06	0.28	100.00	0.00000*	0.6012
	v	7.04	0.31	100.00	0.00000*	
	Downstream	7.00	0.35	100.00	0.00000*	
Synechococcus sp.	Upstream	6.27	0.42	100.00	0.53309	0.00000*
	v	6.41	0.45	100.00	0.62532	
	Downstream	6.52	0.49	100.00	0.34093	
Nanoeukaryotes	Upstream	6.99	0.23	100.00	0.00315*	0.00000*
	v	6.89	0.23	100.00	0.00003*	
	Downstream	6.70	0.26	100.00	0.00004*	
Diatoms	Upstream	3.51	1.55	88.00	0.12217	0.003*
	v	4.27	1.15	99.00	0.00056*	
	Downstream	4.18	1.13	99.00	0.00128*	
Dinoflagellates	Upstream	0.94	1.68	26.00	0.22786	0.00000*
	v	1.70	1.86	49.00	0.00252*	
	Downstream	2.38	1.79	70.00	0.0008*	
Prymnesiophytes	Upstream	0.23	0.96	6.00	insufficient data	0.5193
	v	0.26	1.10	6.00		
	Downstream	0.47	1.45	10.00		
Chlorophytes	Upstream	0.22	1.07	4.00	insufficient data	0.7642
	v	0.24	0.89	7.00		
	Downstream	0.26	0.97	7.00		
Cryptophytes	Upstream	1.04	2.00	22.00	0.98708	0.0007*
	v	1.97	2.35	42.00	0.64574	
	Downstream	2.67	2.26	59.00	0.7442	

TABLE 3 – Block and variable importance (mean % [IC]_{95%}) obtained by (K+1) multiblock method on phytoplankton group abundances. * indicates significant percentages ($p < 0.05$, bootstrap simulations, $N=5000$). (Temp: temperature; PAR: Photosynthetically Active Radiations; Sal: salinity; Turb: turbidity; NO₃: Nitrates; Si: Silica; N/P: Nitrates/Phosphates; PO₄: Phosphates; Si/N: Silica/Nitrates; NH₄: Ammonia; Cu: Copper; Ni: Nickel; Cd: Cadmium; Zn: zinc).

Block	Block importance (%)	IC-95%	Variable	Variable importance (%)	IC-95%
Physical environment	53.1*	[47.1-59]	Temp.	34.4%*	[24.6-44.1]
			PAR	16%*	[10.6-21.3]
			Sal.	14%*	[11-17.1]
			Turb.	9.1%	[5.9-12.2]
Nutrients	27.7	[24.8-30.6]	NO ₃	5%	[3.1-7]
			Si	4.5%	[2.3-6.6]
			N/P	3.6%	[2.1-5.1]
			PO ₄	2.1%	[0.2-4]
			Si/N	2.1%	[1.1-3.1]
			NH ₄	0.8%	[0-1.6]
Metals	19.2	[14.1-24.3]	Cu	2.9%	[0.8-5]
			Ni	2.8%	[0-6]
			Cd	2%	[0.6-3.4]
			Zn	0.8%	[0-2.6]

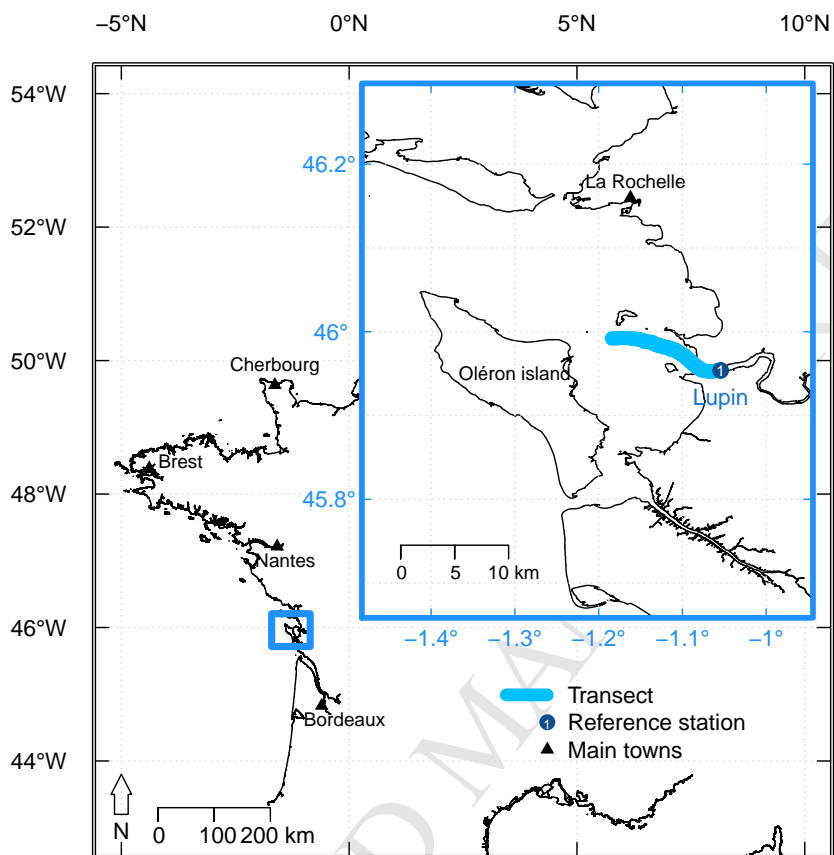


FIGURE 1 – Location of the Charente estuary and Marennes-Oleron basin (blue box) on the French west coast between Nantes and Bordeaux. The blue line represents the sampling transect including the fixed station "Lupin".

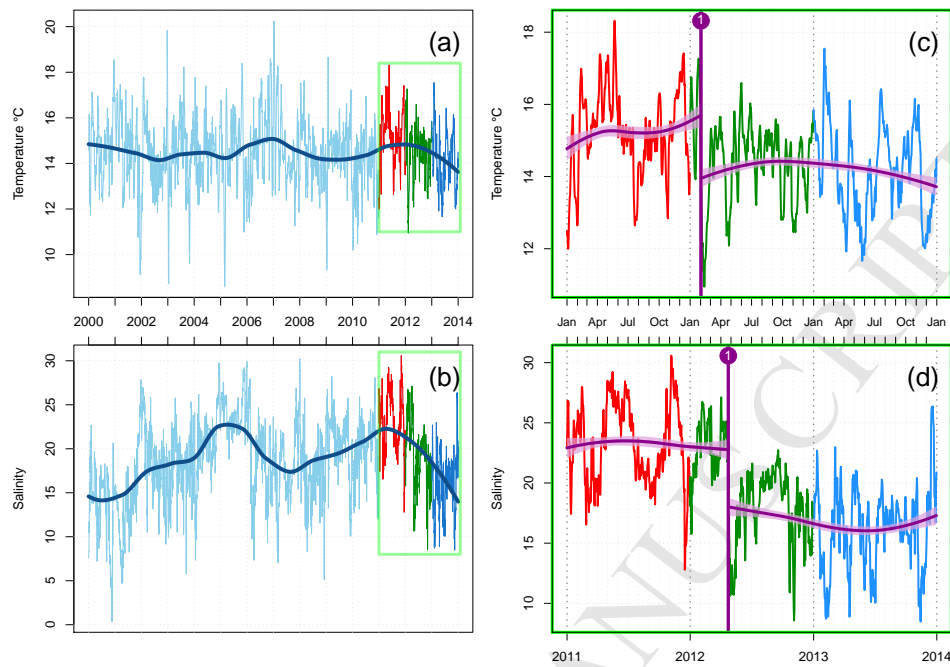


FIGURE 2 – Deseasonalized temperature and salinity at Lupin station from 2000 to 2014 (a and b, respectively) with a fine-scaled view from 2011 to 2014 on the right (c and d, respectively). Vertical lines on parts c and d (labelled with the number one) represent a breakpoint identified in each series. Straight dark blue and purple lines represent smoothed data (loess) (with IC95 on both sides of the break in each series in c and d).

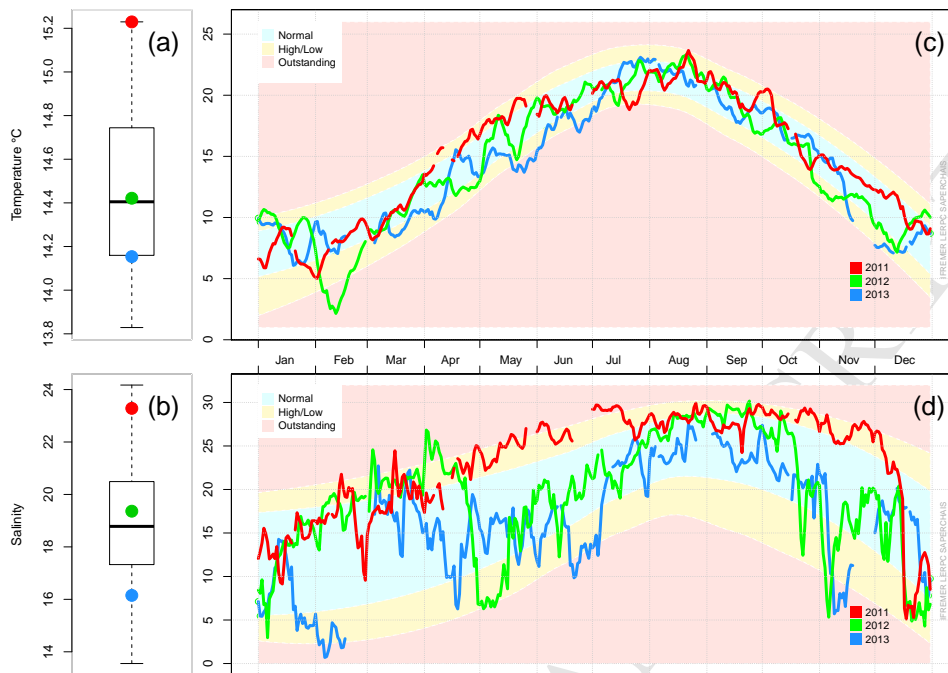


FIGURE 3 – On the left, the positions of annual mean values of temperature (a) and salinity (b) recorded in 2011, 2012 and 2013 are represented on box-plots from data recorded from 2000 to the end of 2013. On the right, daily mean values of temperature (c) and salinity (d) recorded in 2011, 2012 and 2013, are plotted onto the distribution of mean values recorded at Lupin station from 2000 to 2013. The blue area represents values comprised between percentiles 16 and 84, considered as normal data; the yellow areas represent values between percentiles 2.5 and 16 and between percentiles 84 and 97.5, considered as low and high values, respectively; the pink areas represent values lower than percentile 2.5 or higher than percentile 97.5, considered as outlying values.

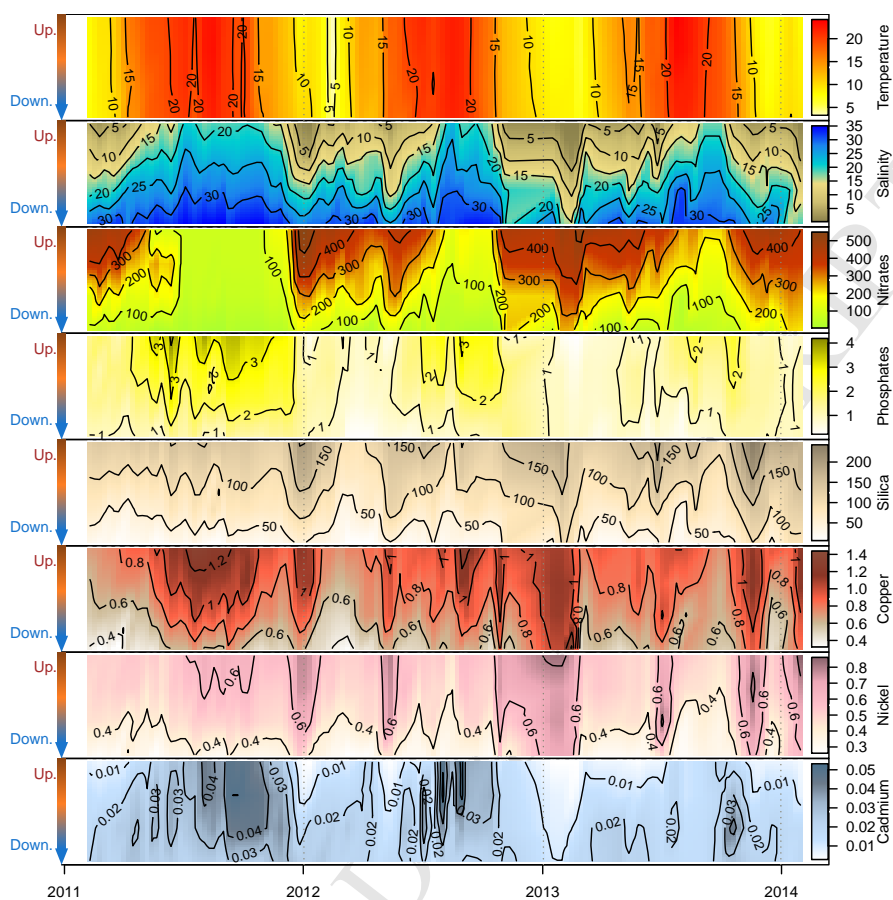


FIGURE 4 – Physical and chemical parameters in the Charente estuary from upstream to downstream (Up and Down, left axes) during the whole study (2011 to 2014). Data scales, represented using isolines and coloured areas, are shown on the right for each parameter: Temperature ($^{\circ}\text{C}$), Salinity, Nitrates (μM), Phosphates (μM), Silica (μM), Copper ($\mu\text{g.L}^{-1}$), Nickel ($\mu\text{g.L}^{-1}$) and Cadmium ($\mu\text{g.L}^{-1}$).

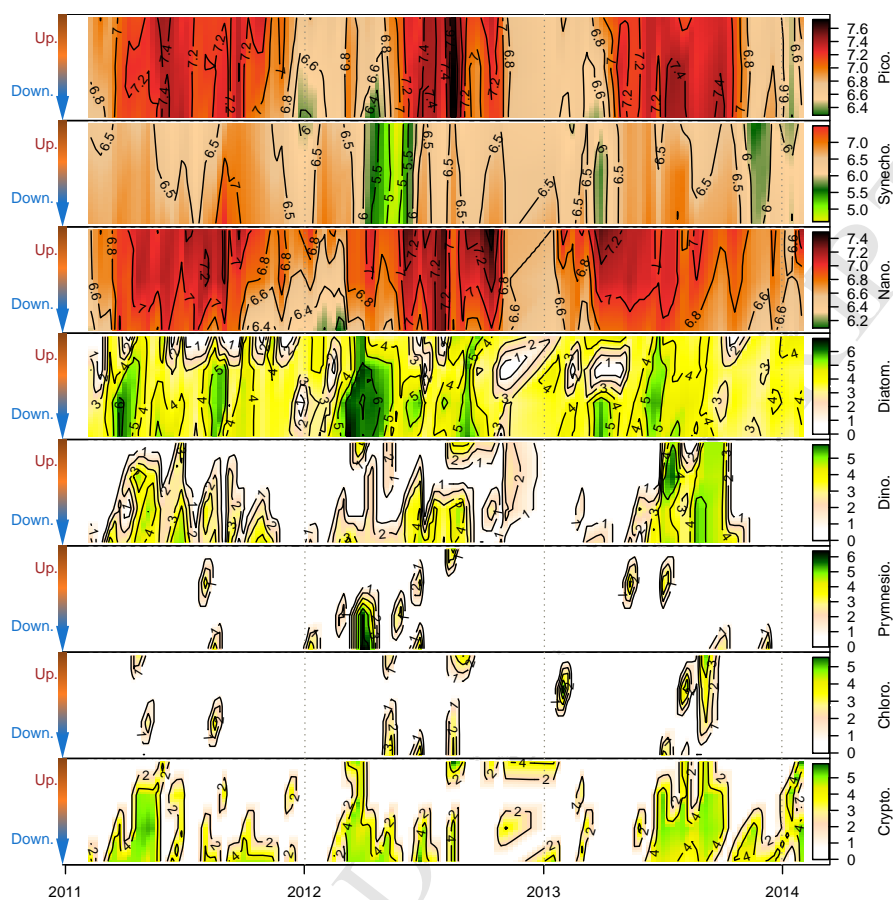


FIGURE 5 – Phytoplankton group abundances ($\text{Log}_{10} \text{ cell.L}^{-1}$) in the Charente estuary from upstream to downstream (Up and Down, left axes) during the whole study (2011 to 2014). Data scales, represented using isolines and coloured areas, are shown on the right for each community (Pico: picoeukaryotes; Synecho: *Synechococcus sp.*; Nano: nanoeukaryotes; Diatom: diatoms; Dino: dinoflagellates; Prymnesio: prymnesiophytes; Chloro: chlorophytes; Crypto: cryptophytes).

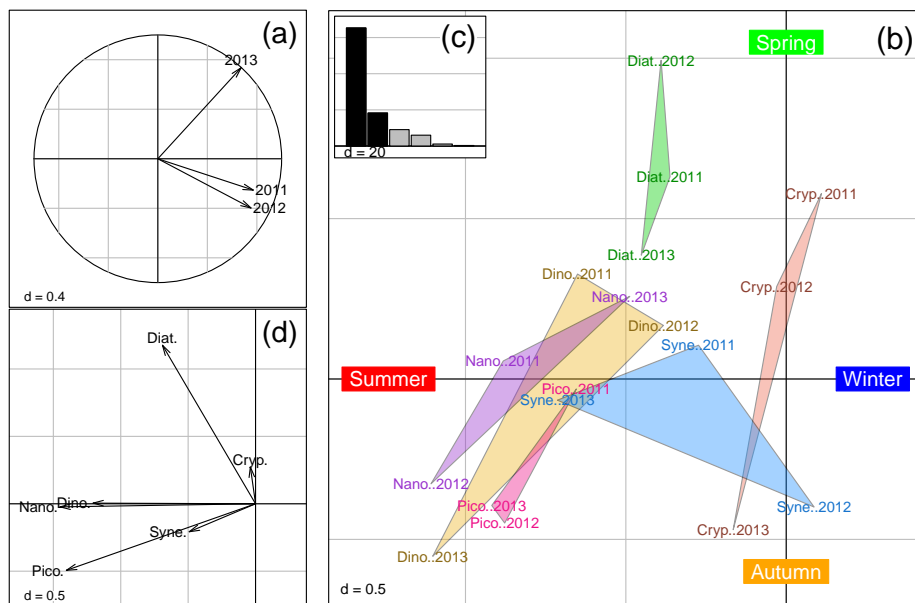


FIGURE 6 – Partial triadic analysis on phytoplankton group abundances during years 2011, 2012 and 2013: (a) interstructure, (b) intrastructure, (c) eigenvalues (projected inertia %) and (d) compromise (Pico: picoeukaryotes; Syne: *Synechococcus sp.*; Nano: nanoeukaryotes; Diat: diatoms; Dino: dinoflagellates; Cryp: cryptophytes).

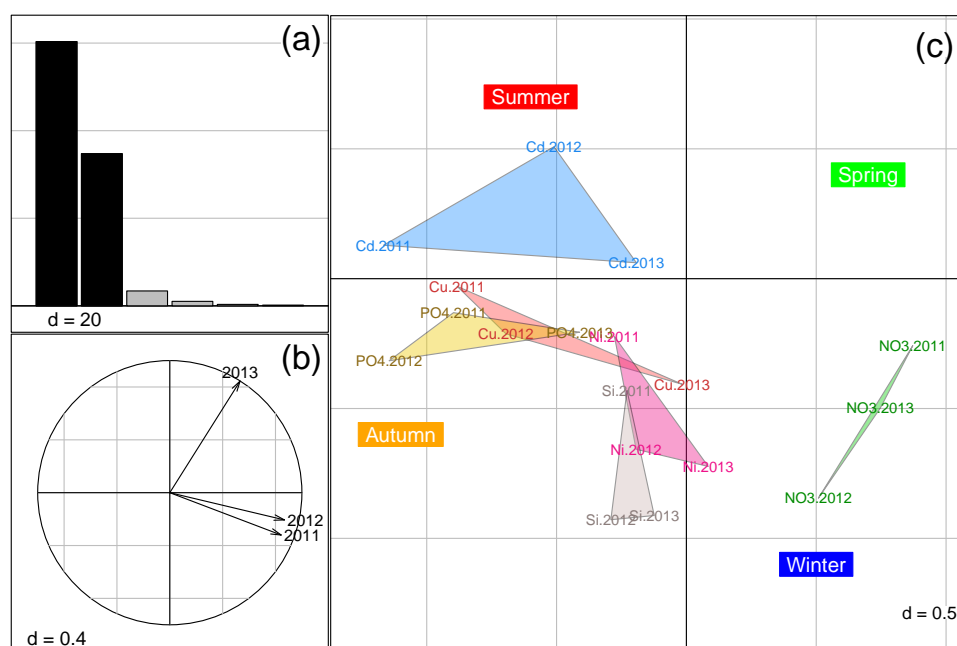


FIGURE 7 – Partial triadic analysis on nutrient and trace element concentrations during years 2011, 2012 and 2013: (a) eigenvalues (projected inertia %), (b) interstructure and (c) intrastructure (Cd: Cadmium; Cu: Copper; Ni: Nickel; NO₃: Nitrates; PO₄: Phosphates; Si: Silica).

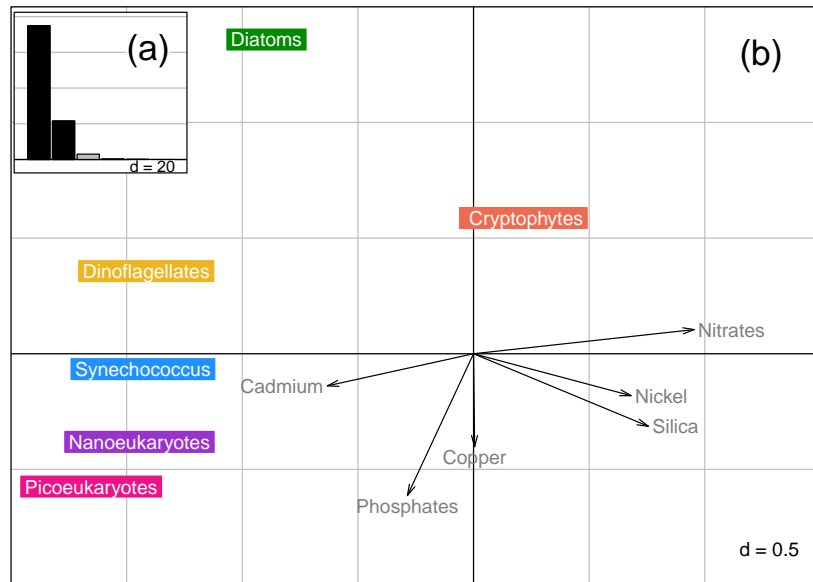


FIGURE 8 – STATICO analysis on phytoplankton group abundances and nutrients and trace elements during years 2011, 2012 and 2013: (a) eigenvalues (projected inertia %), (b) compromise.